

## Short communication

Microstructure and electrical properties of  
 $\text{Pr}_6\text{O}_{11}\text{--Co}_3\text{O}_4\text{--MnCO}_3\text{--Y}_2\text{O}_3$ -doped ZnO varistorsMao-hua Wang<sup>\*</sup>, Gang Li, Chao Yao*School of Chemistry and Chemical Engineering, Changzhou University, Jiangsu, Changzhou 213164, PR China*

Received 2 August 2010; received in revised form 10 December 2010; accepted 8 March 2011

Available online 14 April 2011

**Abstract**

The microstructure and electrical properties of the ZPCMY varistor ceramics composed of  $\text{ZnO--Pr}_6\text{O}_{11}\text{--Co}_3\text{O}_4\text{--MnCO}_3\text{--Y}_2\text{O}_3$  systems sintered at temperature of 1200–1300 °C were investigated. The addition of  $\text{Y}_2\text{O}_3$  led to the decrease of the densification and the slight improvement of the electrical properties. The varistor voltage decreased over a wide range from 7100 to 2470 V/cm with the increase of sintering temperature. The ZPCMY-based varistor ceramics sintered at 1275 °C exhibited the best performance in terms of the densification and  $E\text{--}J$  characteristics. These varistors were characterized by 5.27 in bulk density, 55.3 in the nonlinear exponent and 1.53  $\mu\text{A}$  in the leakage current. © 2011 Elsevier Ltd and Techna Group S.r.l. All rights reserved.

**Keywords:** C. Electrical properties; E. Varistors; Microstructure;  $\text{Pr}_6\text{O}_{11}$

**1. Introduction**

ZnO varistors are polycrystalline ceramics used as surge absorber in electronic circuits, devices and electrical power systems to protect from transitory overvoltage. Their primary property is high nonlinear voltage ( $E$ )–current ( $J$ ) characteristics, often expressed by  $I = KV^\alpha$ , where  $\alpha$  is the nonlinear exponent and  $K$  is a constant that is related with the microstructure, specifically the ZnO grain size. ZnO varistors are usually manufactured in solid state from ZnO particles with small amount of doping agent oxides, such as  $\text{Bi}_2\text{O}_3$ ,  $\text{Sb}_2\text{O}_3$ ,  $\text{CoO}$ ,  $\text{Mn}_2\text{O}_3$ , and  $\text{Cr}_2\text{O}_3$  [1,2]. The mixed powder then being pressed and sintered at high temperature. Small amounts of oxide are added to control the electrical characteristics of the ZnO grain boundaries, and to optimize the varistor behavior. Three significant parameters characterized the varistors, namely the nonlinear exponent  $\alpha$ , the varistor voltage  $E_{1\text{mA}}$  and the leakage current  $J_L$ . The basic building block of the varistor microstructure consists of matrix of ZnO grains surrounded by grain boundaries providing p–n junction semiconductor characteristic. The nonlinear properties of

ZnO varistors result from a double Schottky barrier formed at these active grain boundaries comprising many trap states.

In recent years,  $\text{Pr}_6\text{O}_{11}$ -added ZnO varistors with various dopants of rare-earth oxides (REOs), such as  $\text{Er}_2\text{O}_3$  and  $\text{Dy}_2\text{O}_3$ , are being actively studied aiming to find a substitution for  $\text{Bi}_2\text{O}_3$ -based ZnO varistors, which have some drawbacks due to  $\text{Bi}_2\text{O}_3$  having high volatility and reactivity [3–5]. One of features of  $\text{Pr}_6\text{O}_{11}$ -added ZnO varistors is that the microstructure is simple consisting in two phase only: ZnO grain and intergranular layer. Their nonlinearity can be obtained by doping a few additives. However, they also have some flaws to improve, namely, the high sintering temperature and dissatisfactory performance [6,7]. There have been a number of studies addressing the microstructure, electrical conduction, degradation characteristics, nonlinear properties and mechanisms of ZnO ceramics. It is proved that sintering temperature and nonlinearity of ZnO varistors are directly related to their original grain size and the addition of REO. Therefore, in this paper, the effect of  $\text{Y}_2\text{O}_3$  on the microstructure and electrical properties of the  $\text{ZnO--Pr}_6\text{O}_{11}\text{--Co}_3\text{O}_4\text{--MnCO}_3\text{--Y}_2\text{O}_3$  system was investigated in detail.

**2. Experimental**

Nanocrystalline ZnO powders (purity ~ 99.9%, particle sizes 20–100 nm) used in this study were procured from

<sup>\*</sup> Corresponding author. Tel.: +86 519 81193660.

E-mail address: [wmhj2000@163.com](mailto:wmhj2000@163.com) (M.-h. Wang).

Sinopharm Chemical Co., Inc. Other oxides such as  $\text{Pr}_6\text{O}_{11}$ ,  $\text{Co}_3\text{O}_4$ ,  $\text{MnCO}_3$ , and  $\text{Y}_2\text{O}_3$  were reagent grade. The varistor samples used in this experiment were based on the two compositions: 98 mol%ZnO + 0.5 mol% $\text{Pr}_6\text{O}_{11}$  + 1 mol%- $\text{Co}_3\text{O}_4$  + 0.5 mol%MnCO<sub>3</sub> (designated as ZPCM) and 97.5 mol%ZnO + 0.5 mol% $\text{Pr}_6\text{O}_{11}$  + 1 mol% $\text{Co}_3\text{O}_4$  + 0.5 - mol%MnCO<sub>3</sub>+...+0.5 mol% $\text{Y}_2\text{O}_3$  (designated as ZPCMY). Raw materials were mixed for 24 h in deionized water with zirconia balls and acetone in a polypropylene bottle. The mixture was then dried at 120 °C for 12 h and calcined in air at 750 °C for 2 h. The calcined mixture was again milled for 6 h in the deionized water after 2.5 wt% polyvinyl alcohol (PVA) binder addition. After drying again, the mixture was pulverized using an agate mortar/pestle and granulated using a sieving 200-mesh screen to produce the starting powder. The powder was compacted into discs of 16.66 mm in diameter and 2 mm in thickness by employing a 30 MPa pressure in a uniaxial press. The samples were then sintered at multiple temperatures (1200 °C, 1250 °C, 1275 °C and 1300 °C) for 2 h in air, with heating and cooling rates of rate of 3 °C/min. The sintered samples were lapped and polished to 1.0 mm thickness. Silver paste was coated on both faces of samples and ohmic contact of electrodes was formed by heating at 600 °C for 15 min. The size of electrodes was 13 mm in diameter. The sintered densities ( $\rho$ ) of the green samples were determined by the Archimedes method with distilled water.

For microstructural observations, the either surface was lapped and ground with SiC paper and finally polished with 0.3  $\mu\text{m}$ - $\text{Al}_2\text{O}_3$  powder to mirror-like surface. The polished surfaces were etched with 2% natal (2 vol.% nitric acid with alcohol) for about 1–2 min. The microstructure was examined by scanning electron microscopy (SEM, JSM-6360LA, Japan). The average grain size was measured directly form the micrographs of the etched samples by the lineal intercept method, as described by Mendelson [8],  $G = 1.56L/MN$ , where  $L$  is the random line length on the micrograph,  $M$  is the magnification of the micrograph, and  $N$  is the number of the grain boundaries intercepted by lines. The phases were identified by X-ray diffraction techniques (XRD, D/max 2500 PC, Japan) using a Cu K $\alpha$  radiation.

For electrical measurements, the current–voltage ( $E$ – $J$ ) characteristics were determined at room temperature using a variable DC power supply. The varistor voltage ( $E_{1\text{mA}}$ ) was measure at 1.0 mA/cm<sup>2</sup> and the leakage current ( $J_L$ ) was defined as the current at  $0.83E_{1\text{mA}}$ . The nonlinear exponent ( $\alpha$ ) is defined by  $\alpha = (\log J_2 - \log J_1)/(\log E_2 - \log E_1)$ , where  $E_1$  and  $E_2$  are the electric fields responding to  $J_1 = 0.1 \text{ mA/cm}^2$  and  $J_2 = 1 \text{ mA/cm}^2$ .

### 3. Results and discussion

Fig. 1 presents the variation of bulk density of ZPCM and ZPCMY samples as a function of sintering temperature for 2 h. It can be seen that the sintered densities for both systems increased as sintering temperature increased. However, the sintered densities of all ZPCMY samples are slightly lower than those of ZPCM samples at the same sintering temperature. This

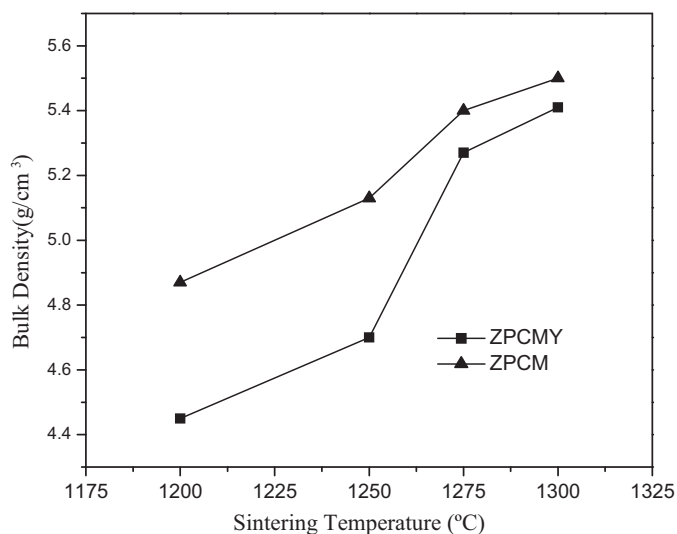


Fig. 1. The bulk density of ZPCM and ZPCMY samples as a function of sintering temperature.

could be related to the addition of  $\text{Y}_2\text{O}_3$ . The  $\text{Y}_2\text{O}_3$  did not impact the densification of ZnO varistor ceramics. This result agrees well with Nahm et al. [9].

Figs. 2 and 3 respectively show scanning electron microscope (SEM) images of ZPCM and ZPCMY polished and etched samples for different sintering temperatures. These figures show that the grain boundaries are visible. The  $\text{Y}_2\text{O}_3$  additive influence on the microstructure is significant. The structure of ZPCMY samples look loosened, with distinct globular or elliptical shape particles on the sintered surface. The average grain size was observed to increase from approximately 3.2  $\mu\text{m}$  to 5.5  $\mu\text{m}$  of ZPCM samples and 2.6  $\mu\text{m}$  to 4.1  $\mu\text{m}$  of ZPCMY samples with increasing temperature in the range of 1200–1300 °C. It is believed that the decrease of the grain size of ZPCMY samples is attributed to segregation of  $\text{Y}_2\text{O}_3$ , which is nearly insoluble in ZnO grains, to grain boundaries. This was nearly equal to those of ceramics doped with other rare-earth metal oxides [10].

In Fig. 4 the results of applied electric field vs current density ( $E$ – $J$ ) curves measurements at room temperature for ZPCMY samples are presented. The samples show the electrical conduction characteristics divided into two regions: a linear  $E$ – $J$  relation before the critical operation field and a nonlinear  $E$ – $J$  relation after the critical operation field. The knee region of  $E$ – $J$  curve of sample sintered at the temperature of 1275 °C is much keener than those of samples at other temperatures. This clearly shows that the ZPCMY varistor ceramics sintered at 1275 °C exhibits the best nonlinear properties. The detail  $E$ – $J$  characteristic parameters are summarized in Table 1.

The varistor voltage ( $E_{1\text{mA/cm}^2}$ ) of ZPCMY samples decreased over a wide range from 7100 V/cm to 2470 V/cm with the increase of sintering temperature. This is attributed firstly to the decrease in the number of grain boundaries caused by the increase in the ZnO grain size, and secondly, to the decrease of varistor voltage per grain boundary [11]. However, the samples sintered at 1300 °C exhibited lower varistor voltage, only 2470 V/cm. This can be explained by the much

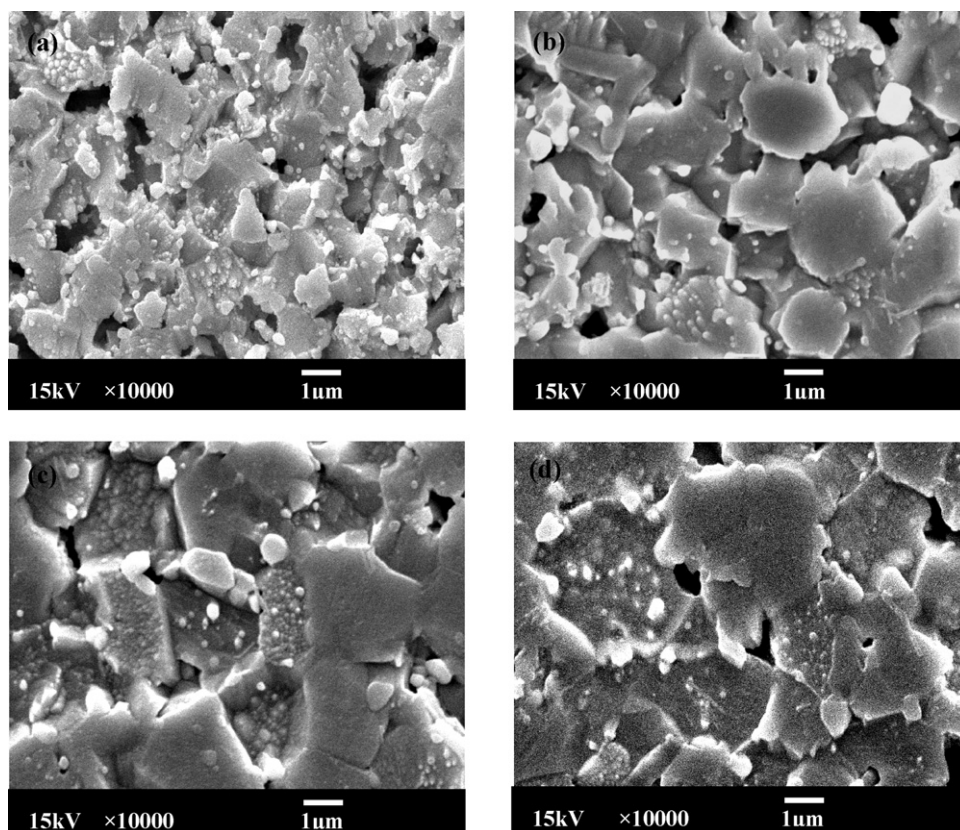


Fig. 2. SEM micrographs of ZPCM samples sintered for 2 h at: (a) 1200 °C, (b) 1250 °C, (c) 1275 °C and (d) 1300 °C.

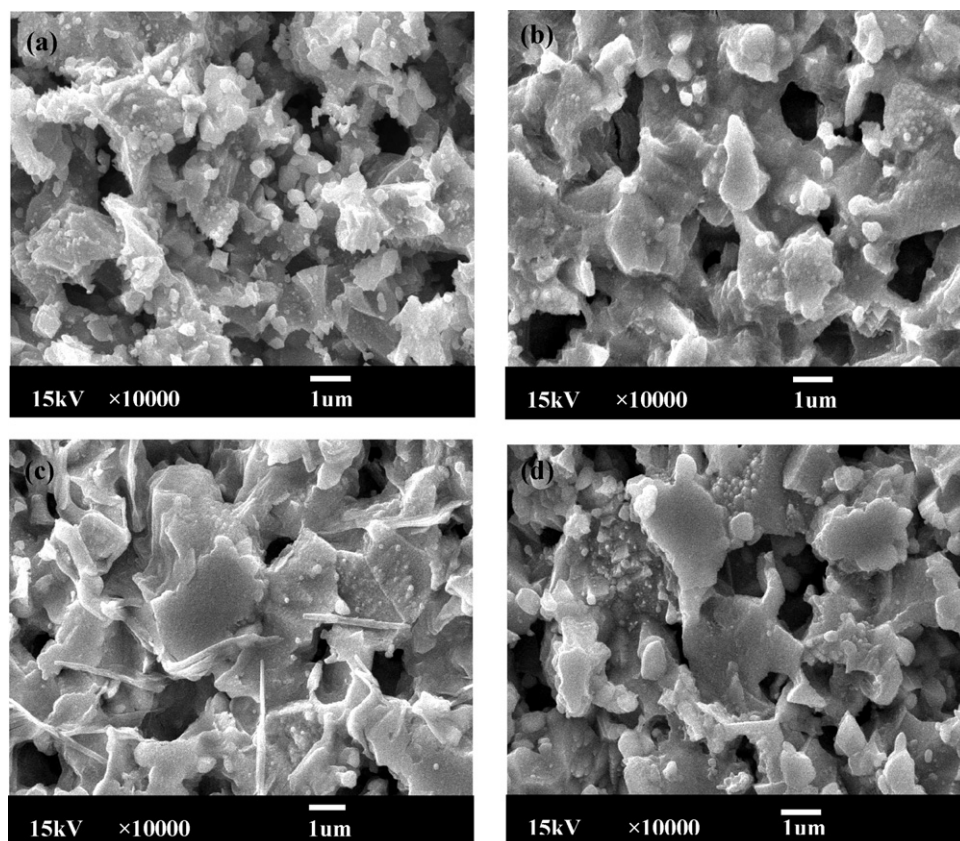


Fig. 3. SEM micrographs of ZPCMY samples sintered for 2 h at: (a) 1200 °C, (b) 1250 °C, (c) 1275 °C and (d) 1300 °C.

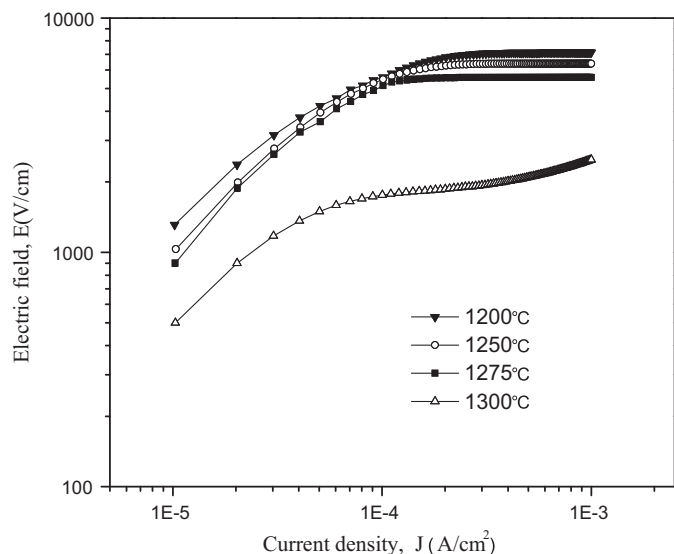


Fig. 4.  $E$ - $J$  characteristics of ZPCMY samples sintered at different temperatures.

lower  $V_{gb}$  value than the general value of 1.5–2.0 V/gb. Therefore, these varistors will exhibit low nonlinear properties.

Fig. 5 shows the nonlinear exponent ( $\alpha$ ) and the leakage current ( $J_L$ ) for different sintering temperatures. The nonlinear exponent ( $\alpha$ ) increased as sintering temperature increased up to 1275 °C. Further increase in sintering temperature caused a decrease in the  $\alpha$  value. At 1275 °C the samples exhibited a highest  $\alpha$  value of 55.3, whereas the  $\alpha$  value abruptly decreased to 6.97 at 1300 °C. This shows that the sintering temperature greatly affects nonlinear properties. These variations of nonlinear properties with sintering temperature are closely related to Schottky barrier at the grain boundary. It is usually the case that the higher barrier height leads to the higher  $\alpha$  [12,13]. While the variation of  $J_L$  value was opposite to that of  $\alpha$  value. This is because the high  $\alpha$  value leads to low leakage current

Table 1

Summary of microstructure and  $E$ - $J$  characteristic parameters for ZPCMY samples sintered at different temperatures.

Sintering temperature (°C)	Sintering time (h)	Average ZnO grain size ( $\mu\text{m}$ )	$E_{1\text{mA}/\text{cm}^2}$ (V/cm)	$E_b$ (V/gb)	Nonlinear exponent ( $\alpha$ )	$J_{\text{leak}}$ ( $\mu\text{A}/\text{cm}^2$ )
1200	2	2.6	7100	1.84	10.8	36.3
1250	2	2.9	6350	1.84	26.6	12.5
1275	2	3.3	5530	1.83	55.3	1.53
1300	2	4.1	2470	1.01	6.97	2.28

due to relatively high tunneling current and the low leakage current due to relatively high thermionic emission current [9].

#### 4. Conclusion

The microstructure and electrical properties of ZnO- $\text{Pr}_6\text{O}_{11}$ - $\text{Co}_3\text{O}_4$ - $\text{MnCO}_3$ - $\text{Y}_2\text{O}_3$ -based varistor ceramics were investigated at different sintering temperatures. The microstructure of ZPCMY-based varistor ceramics was composed of ZnO primary grain and intergranular layer as secondary phases. Compared with the ZPCM samples, the ZPCMY samples became less densified due to the incorporation of rare oxide  $\text{Y}_2\text{O}_3$ . As the sintering temperature increased, the varistor voltage decreased in the range of 7100–2470 V/cm. The nonlinear exponent ( $\alpha$ ) increased as sintering temperature increased up to 1275 °C. Further increase in sintering temperature caused a decrease in the  $\alpha$  value. While the variation of  $J_L$  value was opposite to that of  $\alpha$  value. The ZPCMY-based varistor ceramics sintered at 1275 °C exhibited the best electrical properties, with the nonlinear exponent ( $\alpha$ ) attaining a highest value of 55.3 and a lowest leakage current of 1.53  $\mu\text{A}$ .

#### References

- [1] M. Matsuoka, Nonohmic properties of zinc oxide ceramics, *Jpn. J. Appl. Phys.* 10 (6) (1971) 736–746.
- [2] T.K. Gupta, Application of zinc oxide varistor, *J. Am. Ceram. Soc.* 73 (1990) 1817–1840.
- [3] J. Ott, A. Lorenz, M. Harrier, E.A. Preissner, et al., The influence of  $\text{Bi}_2\text{O}_3$  and  $\text{Sb}_2\text{O}_3$  on the electrical properties of ZnO-based varistors, *J. Electroceram.* 6 (2) (2001) 135–146.
- [4] T. Senda, Grain growth in sintering ZnO and ZnO- $\text{Bi}_2\text{O}_3$  ceramics, *J. Am. Ceram. Soc.* 73 (1990) 106–114.
- [5] A.B. Alles, R. Puskas, G. Callahan, V.L. Burdick, Compositional effect on the liquid-phase sintering of praseodymium oxide-based zinc oxide varistors, *J. Am. Ceram. Soc.* 76 (8) (1993) 2098–2102.
- [6] K. Mukae, Zinc oxide varistors with praseodymium oxide, *Am. Ceram. Soc. Bull.* 66 (1987) 1329–1331.
- [7] C.-W. Nahm, Effect of  $\text{MnO}_2$  addition on microstructure and electrical properties of ZnO- $\text{V}_2\text{O}_5$ -based varistor ceramics, *Ceram. Int.* 35 (2009) 541–546.
- [8] M.I. Mendelson, Lineal intercept for measuring grain size in two-phase polycrystalline ceramics, *J. Am. Ceram. Soc.* 55 (1972) 109–111.
- [9] C.-W. Nahm, B.C. Shin, B.H. Min, Microstructure and electrical properties of  $\text{Y}_2\text{O}_3$ -doped ZnO- $\text{Pr}_6\text{O}_{11}$ -based varistor ceramics, *Mater. Chem. Phys.* 82 (2003) 157–164.

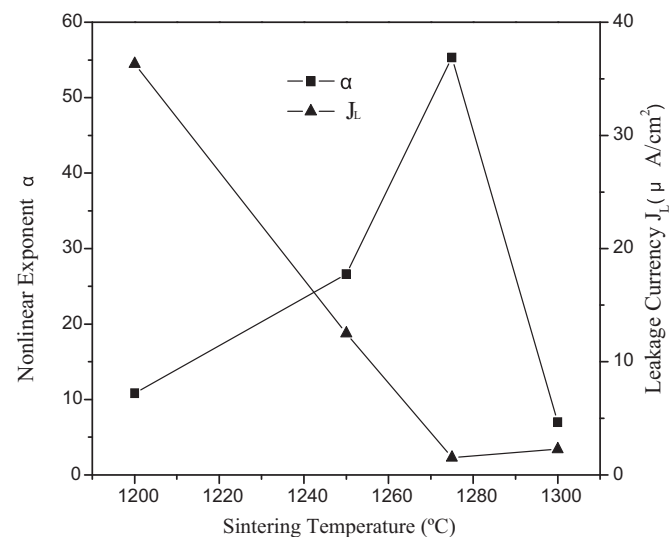


Fig. 5. Nonlinear exponent and leakage current of the ZPCMY samples sintered at different temperatures.

- [10] C.-W. Nahm, The electrical properties and d.c. degradation characteristics of  $\text{Dy}_2\text{O}_3$  doped  $\text{Pr}_6\text{O}_{11}$ -based ZnO varistors, *J. Eur. Ceram. Soc.* 21 (2001) 545–553.
- [11] C.-W. Nahm, The effect of sintering temperature on varistor properties of (Pr, Co, Cr, Y, Al)-doped  $\text{Pr}_6\text{O}_{11}$ ZnO ceramics, *J. Mater. Lett.* 62 (2008) 4440–4442.
- [12] P.R. Bueno, M.R. de Cassia-Santos, E. Leite, E. Longo, J. Bisquert, G. Garcia-Belmonte, et al., Nature of Schottky-type barrier of highly dense  $\text{SnO}_2$  systems displaying nonohmic behavior, *J. Appl. Phys.* 88 (2000) 6545–6548.
- [13] J. Fan, H. Zhao, Y. Xi, Y. Mu, F. Tang, R. Freer, Characterisation of  $\text{SnO}_2$ – $\text{CoO}$ – $\text{MnO}$ – $\text{Nb}_2\text{O}_5$  ceramic, *J. Eur. Ceram. Soc.* 30 (2009) 545–548.